Available online at www.sciencedirect.com

ScienceDirect

Advances in Space Research xx (2021) xxx-xxx

ADVANCES IN SPACE RESEARCH
(a COSPAR publication)

www.elsevier.com/locate/asr

Ionospheric Disturbances in Mexican Territory Produced by Objects Entering the Athmosphere from Space

Jorge Tarango-Yong[a,*], Mario Rodriguez-Martinez[a,**], Raul Gutiérrez-Zalapa[a,1]

[a] *Escuela Nacional de Estudios Superiores, UNAM, campus Morelia, Antigua Carretera a Pátzcuaro No. 8701 Col. Ex Hacienda de San José de la Huerta, Morelia, Michoacán, 58190, México*

Received 1 May 2013; Received in final form 10 May 2013; Accepted 13 May 2013;
Available online 15 May 2013

Abstract

Please type your abstract here, and the rest of the text, figures, tables, equations etc. in the main body. Please do not modify LaTeX commands unless you need to modify them and know how to do it.

Keywords: Space Sciences; Atmosphere

1. Introduction

The Earth's magnetic field represents a final obstacle to the Solar Wind (SW) flux. When descelerated and defected by a non colisional shock wave in the flux direction, generates a cavity known as magnetosphere (Blanco-Cano et al., 2004). Since the Earth is embedded in this SW flux, is known that under adequated physical conditions (e.g magnetic reconnection) may exist some coupling between the magnetosphere and the Earth's ionosphere (Zolesi & Cander, 2014; Cnossen et al., 2012).

The Sun plays an important role in the physical proccesses that occur in the terrestrial magnetosphere-ionosphere system. When the SW interacts with the Earth's magnetosphere, particles may permeate the internal region via magnetic reconnection and penetrate to polar zones and generate boreal or austral auroras thus altering the system (Vázquez et al., 2016; Oka et al., 2011). By the other hand, the Extreme Ultraviolet Radiation (EUV) and X-rays coming from the Sun may interact with the neutral atmoshere via photoionization (Vlasov & Kelley, 2010). However, in both cases the final result is that the ionosphere's free electrons population is altered.

Some Ionospheric Perturbations (IP) become relevant due to their spatial and temporal scale in the Space Weather scenario. At intermediate latitudes, the most common in the ionosphere are known as Traveling Ionospheric Disturbances (TIDs). Typically they divide into two groups: a) large scale TIDs, associated with geomagnetic storms with sizes of $\sim$2000 km, periods of $\sim$1 h and velocities of $\sim$700 km s^{-1}, and b) Medium-scale TIDs, which are not fully associated with geomagnetic storms, present sizes of $\sim$100 km, periods from 10 minutes to 1 hour and velocities between 50 km s^{-1} and 1×10^2 km s^{-1} (Helmboldt et al., 2012). Diverse methods have benn used to study TIDs, such as incoherent dispersion radars, high frequency Doppler emmisors, data from Global Positioning System (GPS) stations or even radiotelescopes like the VLA or the Mexican Array Radio Telescope (MEXART) (Chilcote et al., 2015; Rodríguez-Martínez et al., 2014).

On the other side, the Earth's ionosphere may be affected or modified by other proccesses, particularly there are studies that show how the Vetical Total Electron Content (vTEC) due to shock waves generated for rockets launched to space (Lin et al., 2014). Similar proccesses modify the Earth's ionosphere due to objects entering the athmosphere from space, such as meteoroids like the one which fell on Chelyabinsk at 2013 (Yang et al., 2014). Previously, the ionospheric perturbations pro-

*Tel.: +52-443-476-5525;
email: jorge.tarango@comunidad.unam.mx
**email: m.rodriguez@enesmorelia.unam.mx

https://dx.doi.org/10.1016/j.jasr.xxxx.xx.xxx

duced by this object were studied using two independent methods: a) detecting vTEC pertubations using GPS station near the impact location. And b) a wavelets analysis for detection of ...

In 2020 a meteoroid passed in mexican territory through mexican territory, which also was studied (Sergeeva et al., 2021). The meteoroid was recorded with outdoor cameras in different locations. The trajectory could be estimated, as well as other physical parameters.

In this work we will show a similar analysis for a sample of meteoroids detected in mexican territory by different methods. The first subsample consists in objects detected by the Geostationary Lightning Mapper (GLM) whose sizes are estimated between a few decimeters to meters in diameter (Goodman et al., 2013; Jenniskens et al., 2018; Rumpf et al., 2019). The second subsample will consist in objects detected by ocular witnesses from the American Meteor Society and as comparisson we will include the morelian meteoroid reported in Sergeeva et al. (2021) and the Chelyabinsk event Yang et al. (2014). The paper is arranged in the following way: §2 describes the samples of meteoroids as well of the properties that can be obtained from direct observations. Also describes the GPS data corresponding to the dates and locations where each object was located. §3 shows physical parameters of meteoroids obtained from the observed heights and energies. Finally, section §4 shows the vTEC maps and scintillation indices obtained from GPS observations.

2. Methodology

2.1. Meteors Databases

We selected a sample of meteors which were observed in mexican territory from the Geostationary Lightning Mapper (Goodman et al., 2013). Orignally this project was designed to detect ligthning activity in earth's athmosphere, but has been proven that also can detect bolides entering the athmosphere. The detection comes from two satellites called GOES-16 and GOES-17 orbiting the earth in geostationary orbits. We used the interactive database available at `https://neo-bolide.ndc.nasa.gov/#/`. These data are publicly available and easily downloaded from the same website. For each event we can obtain the recorded trajectory of meteors and the corresponding light curve. THe GLM satellites have an umbral magnitude for detection of -14. At this magnitude, a meteor is considered a bolide, and is expected to be at least decimeter-sized (in diameter) to reach such brightness. In the other hand, too bright meteors will saturate the detectors, and thus, lowering the quality of data. The result of this factors implies that the range in size of the objects in our sample varies in diameter between decimeter to meter size. Each event also has assigned a confidence ratio, from low confidence to high, depending in how bright is the event itself and if the trajectory recorded by GLM ressembles (or not) a straight line. We chose only events whose confidence ratio is high, in oreder to be sure we chose the brightest objects, and thus, in the diameter size of bolides, we favored the meter-sized ones. In table 1 we list the object we chose to do this work, order in chronological order. The columns of the table, from left to right are and ID to enumerate the meteors in the sample, the date and time each meteor was detected, the duration of the detection, their respective coordinates and the estimated height of the meteor over the ground at the time of the detection. GOES-16 and GOES-17 systematically detect the meteors at slightly different positions and at slightly different times, so we calculated the mean of the duration, latitude and longitude reported by both satellites for each event, and used the standard deviation as the uncertainties.

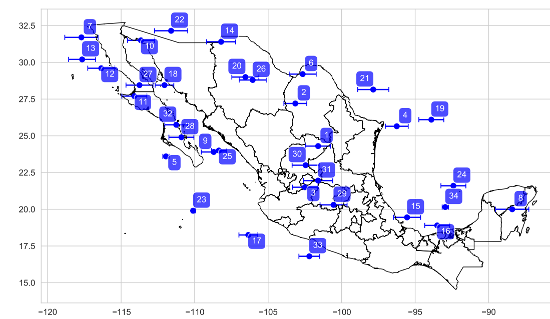

Fig. 1. Positions of events from table 1. The label of each point correspond to the ID (first column) of the referred table.

From table 1 is also clear that the duration of all the bolides detection last less than a second. This obsevation suggests that the bolides remain undetected by the GLM satellites until they get fragmented due to stagnation presure when they release a huge amount of energy and thus they become detectable.

2.2. GPS data

This material is based on services provided by the GAGE Facility, operated by UNAVCO, Inc., with support from the National Science Foundation and the National Aeronautics and Space Administration under NSF Cooperative Agreement EAR-1724794.

We got RINEX data from 3 to 7 stations depending of the event location and data availability that surround the event place in all directions as possible. A list of the stations where we got RINEX data is available in table 2. Most of the stations lie in mexican territory, but in some cases we required data from other stations to cover events near the mexican frontier at north or south.

Table 1. List of meteors passing through Mexico. The events are listed in chronological order. The listed duration, latitude and longitude correspond to the mean of the measurements of both GOES satellites. The uncertainties correspond to the respecting mean deviation.

ID	Date of event	Start Time (UT)	Duration (seconds)	Latitude (deg)	Longitude (deg)	Height (km)	Maximum Kp index
GLM-01	2019-05-23	16:36:18	0.197 ± 0.0000	24.30 ± 0.000	-101.60 ± 0.849	28	2
GLM-02	2019-07-18	14:30:30	0.058 ± 0.0000	27.20 ± 0.000	-103.15 ± 0.778	72	1
GLM-03	2019-08-10	11:18:48	0.199 ± 0.0757	21.50 ± 0.000	-102.50 ± 0.849	92	3
GLM-04	2019-10-03	07:55:33	0.106 ± 0.0297	25.65 ± 0.071	-96.25 ± 0.778	74	2
GLM-05	2019-10-09	06:08:11	0.103 ± 0.0078	23.60 ± 0.000	-111.95 ± 0.212	32	4
GLM-06	2019-11-16	09:36:04	0.396 ± 0.0134	20.30 ± 0.000	-100.55 ± 0.919	82	2
GLM-07	2019-11-17	15:36:01	0.116 ± 0.0035	31.70 ± 0.000	-117.70 ± 1.131	88	3
GLM-08	2019-11-19	07:57:40	0.097 ± 0.1138	20.00 ± 0.000	-88.40 ± 1.131	99	1
GLM-09	2019-11-26	13:23:20	0.078 ± 0.0290	23.90 ± 0.000	-108.70 ± 0.849	81	2
GLM-10	2019-12-04	09:42:54	0.173 ± 0.0028	31.50 ± 0.000	-113.65 ± 0.919	77	2
GLM-11	2019-12-15	14:50:49	0.127 ± 0.0134	27.70 ± 0.000	-114.10 ± 0.849	78	2
GLM-12	2019-12-29	16:16:35	0.062 ± 0.0134	29.60 ± 0.000	-116.35 ± 0.919	79	1
GLM-13	2020-01-03	14:10:17	0.113 ± 0.0085	30.20 ± 0.000	-117.65 ± 0.919	74	3
GLM-14	2020-01-06	16:39:27	0.118 ± 0.0042	31.40 ± 0.000	-108.20 ± 0.990	81	4
GLM-15	2020-01-15	15:00:33	0.213 ± 0.1351	19.45 ± 0.071	-95.55 ± 0.919	93	2
GLM-16	2020-02-12	09:25:40	0.210 ± 0.0226	18.90 ± 0.000	-93.50 ± 0.849	90	2
GLM-17	2020-03-03	12:33:27	0.062 ± 0.0007	18.25 ± 0.071	-106.35 ± 0.636	77	2[2]
GLM-18	2020-03-31	19:31:52	0.105 ± 0.0573	28.45 ± 0.071	-112.05 ± 0.636	61	4
GLM-19	2020-04-08	16:25:28	0.120 ± 0.0926	26.10 ± 0.000	-93.90 ± 0.849	78	3
GLM-20	2020-04-18	17:43:25	0.139 ± 0.0106	29.00 ± 0.000	-106.55 ± 0.919	82	2
GLM-21	2020-04-20	16:05:22	0.318 ± 0.1655	28.15 ± 0.071	-97.85 ± 1.061	88	5
GLM-22	2020-04-25	11:03:09	0.323 ± 0.0813	32.15 ± 0.071	-111.60 ± 1.131	84	3
GLM-23	2020-04-28	19:31:52	0.105 ± 0.0573	28.45 ± 0.071	-112.05 ± 0.636	29	3
GLM-24	2020-05-08	10:06:16	0.490 ± 0.0750	21.60 ± 0.000	-92.40 ± 0.849	81	1
GLM-25	2020-07-15	19:58:28	0.693 ± 0.0495	24.00 ± 0.000	-108.35 ± 0.495	53	2[1]
GLM-26	2020-08-07	13:29:57	0.163 ± 0.0057	28.80 ± 0.000	-106.05 ± 0.919	89	2
GLM-27	2020-09-13	16:41:59	0.184 ± 0.0078	28.45 ± 0.071	-113.75 ± 0.919	85	3
GLM-28	2020-09-30	12:28:11	0.100 ± 0.0078	24.90 ± 0.000	-110.90 ± 0.849	83	4
GLM-29	2020-11-16	12:28:11	0.100 ± 0.0078	24.90 ± 0.000	-110.90 ± 0.849	06	1
GLM-30	2020-11-17	12:53:41	0.404 ± 0.0262	23.00 ± 0.000	-102.45 ± 0.919	93	1
GLM-31	2020-12-19	10:18:14	0.407 ± 0.0110	21.95 ± 0.071	-101.60 ± 0.990	98	2
GLM-32	2020-12-23	09:43:01	0.148 ± 0.0014	25.75 ± 0.071	-111.25 ± 0.778	81	4
GLM-33	2020-12-29	15:20:54	0.118 ± 0.0014	16.80 ± 0.000	-102.20 ± 0.707	81	3
GLM-34	2021-03-31	09:01:17	0.753 ± 0.3083	20.15 ± 0.071	-92.95 ± 0.212	24	3

[1] Kp index is 4 the previous day of impact

[2] Kp index is 4 two days before the impact

Table 2: List of GPS stations used for this work.

Station name	Latitude	Longitude	Events ID			Citation
BAR1[15]	33.48	-119.03	GLM-07	GLM-12	GLM-13	UNAVCO Community, Hudnut, Kenneth, King, Nancy, Aspiotes, Aris G., Borsa, Adrian A., Determan, Daniel N., Galetzka, John E., Stark, Keith F., 2005, SCIGN-PBO Nucleus GPS Network - BAR1-Santa Barbara Island One P.S., The GAGE Facility operated by UNAVCO, Inc., GPS/GNSS Observations Dataset, `https://doi.org/10.7283/T5668BHN`.
BLYT[1]	33.61	-114.71	GLM-12	GLM-13		Hudnut, Kenneth, King, Nancy, Aspiotes, Aris G., Borsa, Adrian A., Determan, Daniel N., Galetzka, John E., Stark, Keith F., 2006, SCIGN USGS GPS Network - BLYT-Blythe P.S., The GAGE Facility operated by UNAVCO, Inc., GPS/GNSS Observations Dataset, `https://doi.org/10.7283/T5HT2MKK`.
CN23	17.26	-88.78	GLM-08	GLM-15	GLM-16	UNAVCO Community, 2012, COCONet GPS Network - CN23-BelmopanBZCR2012 P.S., The GAGE Facility operated by UNAVCO, Inc., GPS/GNSS Observations Dataset, `https://doi.org/10.7283/T5Q23XJH`.
CN25	16.23	-92.13	GLM-15			UNAVCO Community, 2014, COCONet GPS Network - CN25-ComitandDMEX2012 P.S., The GAGE Facility operated by UNAVCO, Inc., GPS/GNSS Observations Dataset, `https://doi.org/10.7283/T57W69G7`.
GCFS	19.31	-81.18	GLM-08			Watts, Anthony, 2016, COCONet GPS Network - GCFS-G_CAYMAN_CYM2014 P.S., The GAGE Facility operated by UNAVCO, Inc., GPS/GNSS Observations Dataset, `https://doi.org/10.7283/7ETV-X536`.
GMPK[1]	33.05	-114.83	GLM-10			UNAVCO Community, Hudnut, Kenneth, King, Nancy, Aspiotes, Aris G., Borsa, Adrian A., Determan, Daniel N., Galetzka, John E., Stark, Keith F., 2005, SCIGN-PBO Nucleus GPS Network - GMPK-Glamis Peak P.S., The GAGE Facility operated by UNAVCO, Inc., GPS/GNSS Observations Dataset, `https://doi.org/10.7283/WCHN-H687`.
GUAT[2]	14.59	-90.52	GLM-16			DeMets, Charles, Cosenza-Muralles, Beatriz, 2021, Central America 2018 - Guatemala, The GAGE Facility operated by UNAVCO, Inc., GPS/GNSS Observations Dataset, `https://doi.org/10.7283/KH2R-K704`.
GUAX[1]	28.88	-118.29	GLM-05 GLM-12 GLM-25 GLM-32	GLM-07 GLM-13 GLM-27	GLM-11 GLM-18 GLM-28	Hudnut, Kenneth, King, Nancy, Aspiotes, Aris G., Borsa, Adrian A., Determan, Daniel N., Galetzka, John E., Stark, Keith F., 2001, SCIGN USGS GPS Network - GUAX-Isla Guadalupe P.S., The GAGE Facility operated by UNAVCO, Inc., GPS/GNSS Observations Dataset, `https://doi.org/10.7283/T5GX48T2`.
IAGX	29.03	-113.17	GLM-10			Gonzalez-Ortega, Alejandro, Galetzka, John E., Gonzalez, Javier, 2018, CICESE REGNOM GPS Network - IAGX-iagxREGNOMmx2018 P.S., The GAGE Facility operated by UNAVCO, Inc., GPS/GNSS Observations Dataset, `https://doi.org/10.7283/DGWN-A627`.
INEG	21.85	-102.28	GLM-25 GLM-29	GLM-26 GLM-30	GLM-28 GLM-31	No citations were found
KVTX	27.55	-97.89	GLM-01 GLM-04 GLM-20 GLM-26	GLM-02 GLM-06 GLM-21	GLM-03 GLM-19 GLM-24	UNAVCO Community, 2007, PBO GPS Network - KVTX-KingsvilleTX2006 P.S., The GAGE Facility operated by UNAVCO, Inc., GPS/GNSS Observations Dataset, `https://doi.org/10.7283/T5J38QH8`.
MDO1	30.68	-104.02	GLM-02			No citations were found
MGO5	30.68	-104.02	GLM-21	GLM-26		No citations were found
MGW3	29.62	-89.95	GLM-19	GLM-21	GLM-24	No citations were found
OXTH	16.29	-95.24	GLM-15	GLM-16		DeMets, Charles, Cabral-Cano, Enrique, 2008, Oaxaca GPS Network - OXTH-Tehuantepec P.S., The GAGE Facility operated by UNAVCO, Inc., GPS/GNSS Observations Dataset, `https://doi.org/10.7283/T5Q81B5V`.
OXUM[3]	15.66	-96.50	GLM-34			Cabral-Cano, Enrique, Salazar-Tlaczani, Luis, 2015, TLALOCNet - OXUM-oxum_tnet_mx2001 P.S., The GAGE Facility operated by UNAVCO, Inc., GPS/GNSS Observations Dataset, `https://doi.org/10.7283/T5J964RP`.
P001	31.95	-112.80	GLM-07	GLM-22		UNAVCO Community, 2008, PBO GPS Network - P001-Organ_PipeAZ2007 P.S., The GAGE Facility operated by UNAVCO, Inc., GPS/GNSS Observations Dataset, `https://doi.org/10.7283/T5DR2SGP`.
P014	31.97	-11.09	GLM-10 GLM-14	GLM-12 GLM-22	GLM-13	UNAVCO Community, 2008, PBO GPS Network - P014-Sahuarita_AZ2007 P.S., The GAGE Facility operated by UNAVCO, Inc., GPS/GNSS Observations Dataset, `https://doi.org/10.7283/T5DJ5CMK`.
P807	30.49	-98.82	GLM-06 GLM-30	GLM-14	GLM-21	UNAVCO Community, 2012, PBO GPS Network - P807-EcRockStPkTX2012 P.S., The GAGE Facility operated by UNAVCO, Inc., GPS/GNSS Observations Dataset, `https://doi.org/10.7283/T5TQ5ZKM`.

PLPX	31.59	-115.15	GLM-10	UNAVCO Community, 2011, PBO GPS Network - PLPX-Las_PintasMX2010 P.S., The GAGE Facility operated by UNAVCO, Inc., GPS/GNSS Observations Dataset, `https://doi.org/10.7283/T5K64G3T`.
PTEX	32.29	-116.52	GLM-07 GLM-12 GLM-13 GLM-27 GLM-32	UNAVCO Community, 2011, PBO GPS Network - PTEX-Testerazo_MX2011 P.S., The GAGE Facility operated by UNAVCO, Inc., GPS/GNSS Observations Dataset, `https://doi.org/10.7283/T5610XBP`.
RG06	32.63	-107.86	GLM-22	Sheehan, Anne, 2007, Rio Grande Rift GPS Network - RG06-RG06FaywodNM2006 P.S., The GAGE Facility operated by UNAVCO, Inc., GPS/GNSS Observations Dataset, `https://doi.org/10.7283/T5668BFR`.
RG07	32.50	-106.84	GLM-14	Sheehan, Anne, 2007, Rio Grande Rift GPS Network - RG07-RG07CrucesNM2006 P.S., The GAGE Facility operated by UNAVCO, Inc., GPS/GNSS Observations Dataset, `https://doi.org/10.7283/T5KD1W45`.
SG33	31.77	-106.51	GLM-06 GLM-20 GLM-26	Harder, Steven, Kaip, Galen, Montana, Carlos, 2004, SuomiNet-G GPS Network - SG33-UTEP P.S., The GAGE Facility operated by UNAVCO, Inc., GPS/GNSS Observations Dataset, `https://doi.org/10.7283/T50863KQ`.
TGMX	20.87	-86.87	GLM-34	UNAVCO Community, 2015, COCONet GPS Network - TGMX-PtoMor_TG_MX2015 P.S., The GAGE Facility operated by UNAVCO, Inc., GPS/GNSS Observations Dataset, `https://doi.org/10.7283/T5154FB7`.
TNAM	20.54	-103.97	GLM-17 GLM-25 GLM-28 GLM-29 GLM-30 GLM-31	UNAVCO Community, 2014, TLALOCNet - TNAM-TNAM_TNET_MX2014 P.S., The GAGE Facility operated by UNAVCO, Inc., GPS/GNSS Observations Dataset, `https://doi.org/10.7283/T5QF8R4R`.
TNAT	18.13	-98.04	GLM-15	UNAVCO Community, 2014, TLALOCNet - TNAT-TNAT_TNET_MX2014 P.S., The GAGE Facility operated by UNAVCO, Inc., GPS/GNSS Observations Dataset, `https://doi.org/10.7283/T5G15Z4S`.
TNBA	28.97	-113.55	GLM-05 GLM-07 GLM-09 GLM-11 GLM-12 GLM-13	UNAVCO Community, 2015, TLALOCNet - TNBA-TNBA_TNET_MX2014 P.S., The GAGE Facility operated by UNAVCO, Inc., GPS/GNSS Observations Dataset, `https://doi.org/10.7283/T57M0688`.
TNCC	18.79	-103.17	GLM-17	UNAVCO Community, 2015, TLALOCNet - TNCC-TNCC_TNET_MX2015 P.S., The GAGE Facility operated by UNAVCO, Inc., GPS/GNSS Observations Dataset, `https://doi.org/10.7283/T50R9MSK`.
TNCM	19.50	-105.04	GLM-17 GLM-23	UNAVCO Community, 2014, TLALOCNet - TNCM-TNCM_TNET_MX2014 P.S., The GAGE Facility operated by UNAVCO, Inc., GPS/GNSS Observations Dataset, `https://doi.org/10.7283/T5B856FW`.
TNCN	18.55	-101.97	GLM-29 GLM-33	UNAVCO Community, 2016, TLALOCNet - TNCN-TNCN_TNET_MX2016 P.S., The GAGE Facility operated by UNAVCO, Inc., GPS/GNSS Observations Dataset, `https://doi.org/10.7283/T5610XQM`.
TNCU	28.45	-106.79	GLM-01 GLM-02 GLM-03 GLM-06 GLM-11 GLM-14 GLM-18 GLM-20 GLM-25 GLM-26 GLM-30 GLM-31	UNAVCO Community, 2014, TLALOCNet - TNCU-CuauhtemocTN2014 P.S., The GAGE Facility operated by UNAVCO, Inc., GPS/GNSS Observations Dataset, `https://doi.org/10.7283/T5V69GV2`.
TNGF	19.33	-99.18	GLM-29 GLM-33	Cabral-Cano, Enrique, Salazar-Tlaczani, Luis, 2016, TLALOCNet GPS Network - TNGF_Geofisica-UNAM_Mexico_City_TNET_mx2015 P.S., The GAGE Facility operated by UNAVCO, Inc., GPS/GNSS Observations Dataset, `https://doi.org/10.7283/T53X851M`.
TNHM	29.08	-110.97	GLM-05 GLM-09 GLM-10 GLM-11 GLM-12 GLM-13 GLM-18 GLM-20 GLM-25 GLM-26 GLM-27 GLM-28 GLM-32	UNAVCO Community, 2014, TLALOCNet - TNHM-hermosilloTN2014 P.S., The GAGE Facility operated by UNAVCO, Inc., GPS/GNSS Observations Dataset, `https://doi.org/10.7283/T5KP80FV`.
TNMS	20.53	-104.80	GLM-05 GLM-09 GLM-11 GLM-17 GLM-25	UNAVCO Community, 2014, TLALOCNet - TNMS-TNMS_TNET_MX2014 P.S., The GAGE Facility operated by UNAVCO, Inc., GPS/GNSS Observations Dataset, `https://doi.org/10.7283/T56H4FQ5`.
TNNP	16.12	-97.14	GLM-23	Cabral-Cano, Enrique, Salazar-Tlaczani, Luis, DeMets, Charles, 2016, TLALOCNet - TNNP-tnnp_tnet_mx2015 P.S., The GAGE Facility operated by UNAVCO, Inc., GPS/GNSS Observations Dataset, `https://doi.org/10.7283/T5N29V96`.
TNNX	17.41	-97.22	GLM-15 GLM-16 GLM-33 GLM-34	UNAVCO Community, 2014, TLALOCNet - TNNX-TNNX_TNET_MX2014 P.S., The GAGE Facility operated by UNAVCO, Inc., GPS/GNSS Observations Dataset, `https://doi.org/10.7283/T52R3PZ0`.
TNPP	31.34	-113.63	GLM-07 GLM-10 GLM-18 GLM-22	UNAVCO Community, 2015, TLALOCNet - TNPP-TNPP_TNET_MX2015 P.S., The GAGE Facility operated by UNAVCO, Inc., GPS/GNSS Observations Dataset, `https://doi.org/10.7283/T5CC0Z0M`.
TNSJ	16.17	-96.49	GLM-33	UNAVCO Community, 2016, TLALOCNet - TNSJ-tnsj_tnet_mx2015 P.S., The GAGE Facility operated by UNAVCO, Inc., GPS/GNSS Observations Dataset, `https://doi.org/10.7283/T59S1PF1`.
TSFX	30.93	-114.81	GLM-07 GLM-27 GLM-32	Gonzalez-Ortega, Alejandro, Galetzka, John E., Gonzalez, Javier, 2018, CICESE REGNOM GPS Network - TSFX-tsfxREGNOMmx2016 P.S., The GAGE Facility operated by UNAVCO, Inc., GPS/GNSS

				Observations Dataset, https://doi.org/10.7283/AGEA-2G27.
UAGU	21.92	-102.32	GLM-01 GLM-02 GLM-03 GLM-04 GLM-06 GLM-09 GLM-11 GLM-20	Cabral-Cano, Enrique, Salazar-Tlaczani, Luis, 2015, TLALOCNet - UAGU-uagu_tnet_mx2008 P.S., The GAGE Facility operated by UNAVCO, Inc., GPS/GNSS Observations Dataset, https://doi.org/10.7283/T5513WK7.
UCOE[3]	19.81	-101.69	GLM-03 GLM-06 GLM-30 GLM-31	Cabral-Cano, Enrique, Salazar-Tlaczani, Luis, 2015, TLALOCNet - UCOE-ucoe_tnet_mx2003 P.S., The GAGE Facility operated by UNAVCO, Inc., GPS/GNSS Observations Dataset, https://doi.org/10.7283/T51834VW.
UGEO[4]	20.69	-103.35	GLM-03	Marquez-Azua, Bertha, DeMets, Charles, Cabral-Cano, Enrique, Salazar-Tlaczani, Luis, 2015, TLALOCNet - UGEO-ugeo_tnet_mx1998 P.S., The GAGE Facility operated by UNAVCO, Inc., GPS/GNSS Observations Dataset, https://doi.org/10.7283/T58S4N9N.
UHSL	29.57	-95.65	GLM-19	Wang, Guoquan, 2014, HoustonNet GPS Network - UHSL-SugarLandUSA2014 P.S., The GAGE Facility operated by UNAVCO, Inc., GPS/GNSS Observations Dataset, https://doi.org/10.7283/T55X271S.
UHWL	30.06	-94.98	GLM-31	Wang, Guoquan, 2014, HoustonNet GPS Network - UHWL-West Liberty Airport(Deep) P.S., The GAGE Facility operated by UNAVCO, Inc., GPS/GNSS Observations Dataset, https://doi.org/10.7283/T53R0R5P.
UNPM	20.86	-86.86	GLM-08 GLM-15 GLM-16 GLM-24	UNAVCO Community, 2012, COCONet GPS Network - UNPM-Puerto_Morelos_MX_2007 P.S., The GAGE Facility operated by UNAVCO, Inc., GPS/GNSS Observations Dataset, https://doi.org/10.7283/J1GD-5S40.
USMX	29.82	-109.68	GLM-12 GLM-13 GLM-14 GLM-22 GLM-26 GLM-28	Bennett, Rick, 2004, Northwest Mexico GPS Network - USMX-Universidad de la Sierra P.S., The GAGE Facility operated by UNAVCO, Inc., GPS/GNSS Observations Dataset, https://doi.org/10.7283/T5W957CQ.
UXAL[3]	19.52	-96.92	GLM-04 GLM-15 GLM-16 GLM-19 GLM-24 GLM-31 GLM-34	Cabral-Cano, Enrique, Salazar-Tlaczani, Luis, 2015, TLALOCNet - UXAL-uxal_tnet_mx2005 P.S., The GAGE Facility operated by UNAVCO, Inc., GPS/GNSS Observations Dataset, https://doi.org/10.7283/T5DJ5D1C.
WEPD	29.69	-95.23	GLM-21	Wang, Guoquan, 2014, HoustonNet GPS Network - WEPD-willmselementary P.S., The GAGE Facility operated by UNAVCO, Inc., GPS/GNSS Observations Dataset, https://doi.org/10.7283/T5NZ85RB.
WMOK	34.74	-98.78	GLM-21	UNAVCO Community, 2005, PBO GPS Network - WMOK-WichitaMtnOK2005 P.S., The GAGE Facility operated by UNAVCO, Inc., GPS/GNSS Observations Dataset, https://doi.org/10.7283/T59021Q6.
WWMT[1]	33.96	-116.65	GLM-07 GLM-12 GLM-13	Hudnut, Kenneth, King, Nancy, Aspiotes, Aris G., Borsa, Adrian A., Determan, Daniel N., Galetzka, John E., Stark, Keith F., 2006, SCIGN USGS GPS Network - WWMT-Whitewater Mountain P.S., The GAGE Facility operated by UNAVCO, Inc., GPS/GNSS Observations Dataset, https://doi.org/10.7283/T5H993F2.
YESX	28.38	-108.92	GLM-09 GLM-11 GLM-14 GLM-20 GLM-23 GLM-25	Bennett, Rick, 2004, Northwest Mexico GPS Network - YESX-Yecora P.S., The GAGE Facility operated by UNAVCO, Inc., GPS/GNSS Observations Dataset, https://doi.org/10.7283/T5RJ4GPF.

Related articles:
[1]Hudnut (2002), [2]Garnier et al. (2021), [3]Graham et al. (2016)
[4]B. Marquez-Azua, E. Cabral-Cano, F. Correa-Mora and C. DeMets, 2004. A model for Mexican neotectonics based on Nationwide GPS measurements, 1993-2001, Geofisica Internacional, v. 43, p.319-330
[5]Hudnut, K. W., Y. Bock, J. E. Galetzka, F. H. Webb, and W. H. Young, The Southern California Integrated GPS Network (SCIGN), Proceedings of the International Workshop on Seismotectonics at the Subduction Zone, Y. Fujinawa (ed.), NIED, Tsukuba, Japan, pp. 175-196, 1999

The obtained RINEX files are compressed in Hatanaka format, developed at the Geographical Survey Institute by Y. Hatanaka (Kumar et al., 2012). From this files we may estimate the Slant Total Electron Content (sTEC) and the Vertical Total Electron Content (vTEC) which may be computed in the following way:

The Total Electron content along the integrated path of the link (s_i) at the frequency f_i can be inferred from the phase delay L_i of the frequency f_i (Emery & Camps, 2017):

$$L_i = s_i - \frac{40.3082\,\mathrm{m}^3\,\mathrm{s}^{-1}}{f_i^2} sTEC_i \tag{1}$$

Combining two observations at two different frequencies f_1 and f_2 we may obtain two different phase delays L_1 and L_2 and derive the TEC along the signal path:

$$sTEC = \frac{f_1^2 f_2^2 (L_1 - L_2)}{40.3082\,\mathrm{m}^3\,\mathrm{s}^{-1}\left(f_1^2 - f_2^2\right)} \tag{2}$$

In the other hand, the Vertical Total Electron Content (vTEC) is computed from the sTEC as follows (Kumar et al., 2012):

$$vTEC = \frac{sTEC - [b_R + b_S]}{S(\theta_I)} \tag{3}$$

where b_R and b_S are receiver and satellite biases, respectively. θ_I is the elevation angle in degrees, $S(\theta_I)$ is the obliquity factor with zenith angle ψ at the Ionospheric Pierce Point (IPP):

$$S(\theta_i) = \frac{1}{\cos\psi} = \left\{1 - \frac{R_E \cos\theta_I}{R_E + h}\right\}^{-1/2} \tag{4}$$

Where R_E is the Earth radius in km and $h = 350\,\mathrm{km}$ is the ionospheric shell above the earth's surface.

Both parameters sTEC and vTEC are computed using a software developed by Gopi K. Seemala, publicly available at `https://seemala.blogspot.com/`.

3. Bolides physical parameters

Enter Raul's work here

4. Ionospheric background and vTEC maps

Ionospheric perturbations also can take place due to space weather and geomagnetic storms. So, in order to discard such events we investigated the space weather in the day each event occured. In figure (name) we present the geomagnetic *Kp* index for some events. We discarded events whose Kp index is equal or grater than 4 in the day of the event or shortly before. Also we present in figure (name) the vTEC perturbation maps for the same events in a three day series, centered in the event date. The estimated meteor trajectory, obtained from the GLM data is presented in black, continous line, while the linear fit to the GOES-16 and GOES-17 data are presented with the red dashed line, and work as boudary errors.

5. Discussion

Enter discussion here

6. Acknowledgments

The RINEX data used in this paper were obtained from the Trans-boundary, Land and Atmosphere Long-term Observational and Collaborative Network (TLALOCNet, Cabral-Cano et al. (2018)), operated by the Servicio de Geodesia Satelital (SGS) at the Instituto de Geofísica-Universidad Nacional Autónoma de México (UNAM) in collaboration with UNAVCO Inc.

We are deeply grateful to all personnel from SGS, SSN and UNAVCO for station installation, maintenance, data acquisition, IT support and data curation and distribution for these networks and in particular to the following individuals and institutions, and those whose hard field work and resourcefulness were central to the success of this project: Bill Douglass, Neal Lord and Bill Unger at UW-Madison, Oscar Diaz-Molina and Luis Salazar-Tlaczani at SGS, John Galetzka, Adam Wallace, Shawn Lawrence, Sean Malloy and Chris Walls at UNAVCO, Jesus Pacheco-Martínez at Universidad Autónoma de Aguascalientes, Bertha Marquez-Azúa and personnel at the Universidad de Guadalajara at campus Guadalajara, Mascota and Ameca, Protección Civil de Jalisco, Universidad de Colima at campus Colima and campus El Naranjo and Centro de Geociencias, Centro de Ciencias de la Atmosfera Instituto de Biología Estacion Chamela at UNAM. TLALOCNet, SSN-TLALOCNet and other GPS related operations from SGS are supported by CONACyT projects 253760, 256012 and 2017-01-5955, UNAM-PAPIIT projects IN104213, IN111509, IN109315-3, IN104818-3, NSF grant 2025104, NASA-ROSES grant NNX12AQ08G and supplemental support from UNAM-Instituto de Geofísica. UNAVCO's initial support for TLALOCNet (some of its stations now part of the GAGE Facility-NOTA) was performed under EAR-1338091 and is currently supported by NSF and NASA under NSF Cooperative Agreement EAR-1724794.

Also we are grateful with the Dirección General de Asuntos Académicos (DGAPA) of the Universidad Nacional Autónoma de México and the Programa de Becas Posdoctorales for funding this project.

References

Blanco-Cano, X., Omidi, N., & Russel, C. T. (2004). How to make a magnetosphere. *Astronomy & Geophysics*, *45*(3), 3.14–3.17. doi:`10.1046/j.1468-4004.2003.45314.x`. `arXiv:https://academic.oup.com/astrogeo/article-pdf/45/3/3.14/193`

Cabral-Cano, E., Pérez-Campos, X., Márquez-Azúa, B., Sergeeva, M. A., Salazar-Tlaczani, L., DeMets, C., Adams, D., Galetzka, J., Hodgkinson, K., Feaux, K., Serra, Y. L., Mattioli, G. S., & Miller, M. (2018). TLALOCNet: A Continuous GPS-Met Backbone in Mexico for Seismotectonic and Atmospheric Research. *Seismological Research Letters*, *89*(2A), 373–381. doi:`10.1785/0220170190`.

Chilcote, M., LaBelle, J., Lind, F. D., Coster, A. J., Miller, E. S., Galkin, I. A., & Weatherwax, A. T. (2015). Detection of traveling ionospheric disturbances by medium-frequency doppler sounding using am radio transmissions. *Radio Science*, *50*(3), 249–263. doi:`https://doi.org/10.1002/2014RS005617`.

Cnossen, I., Wiltberger, M., & Ouellette, J. E. (2012). The effects of seasonal and diurnal variations in the earth's magnetic dipole orientation on solar wind–magnetosphere-ionosphere coupling. *Journal of Geophysical Research: Space Physics*, *117*(A11). doi:`https://doi.org/10.1029/2012JA017825`.

Emery, W., & Camps, A. (2017). Chapter 6 - remote sensing using global navigation satellite system signals of opportunity. In W. Emery, & A. Camps (Eds.), *Introduction to Satellite Remote Sensing* (p. 455–564). Elsevier. URL: `https://www.sciencedirect.com/science/article/pii/B9780128092545000063`. doi:`10.1016/B978-0-12-809254-5.00006-3`.

Garnier, B., Tikoff, B., Flores, O., Jicha, B., DeMets, C., Cosenza-Muralles, B., Hernandez, D., Marroquin, G., Mixco, L., & Hernandez, W. (2021). An integrated structural and GPS study of the Jalpatagua fault, southeastern Guatemala. *Geosphere*, *17*(1), 201–225. doi:`10.1130/GES02243.1`.

Goodman, S. J., Blakeslee, R. J., Koshak, W. J., Mach, D., Bailey, J., Buechler, D., Carey, L., Schultz, C., Bateman, M., McCaul, E., & Stano, G. (2013). The goes-r geostationary lightning mapper (glm). *Atmospheric Research*, *125-126*, 34–49. doi:`https://doi.org/10.1016/j.atmosres.2013.01.006`.

Graham, S., DeMets, C., Cabral-Cano, E., Kostoglodov, V., Rousset, B., Walpersdorf, A., Cotte, N., Lasserre, C., McCaffrey, R., & Salazar-Tlaczani, L. (2016). Slow Slip History for the MEXICO Subduction Zone: 2005 Through 2011. *Pure and Applied Geophysics*, *173*(10-11), 3445–3465. doi:`10.1007/s00024-015-1211-x`.

Helmboldt, J. F., Lane, W. M., & Cotton, W. D. (2012). Climatology of midlatitude ionospheric disturbances from the very large array low-frequency sky survey. *Radio Science*, *47*(5). doi:`https://doi.org/10.1029/2012RS005025`.

Hudnut, K. W. (2002). Continuous GPS Observations of Postseismic Deformation Following the 16 October 1999 Hector Mine, California, Earthquake (Mw 7.1). *The Bulletin of the Seismological Society of America*, *92*(4), 1403–1422. doi:10.1785/0120000912.

Jenniskens, P., Albers, J., Tillier, C. E., Edgington, S. F., Longenbaugh, R. S., Goodman, S. J., Rudlosky, S. D., Hildebrand, A. R., Hanton, L., Ciceri, F., Nowell, R., Lyytinen, E., Hladiuk, D., Free, D., Moskovitz, N., Bright, L., Johnston, C. O., & Stern, E. (2018). Detection of meteoroid impacts by the geostationary lightning mapper on the goes-16 satellite. *Meteoritics & Planetary Science*, *53*(12), 2445–2469. doi:https://doi.org/10.1111/maps.13137.

Kumar, D. S., Priyadarshi, S., Seemala, G., & Singh, A. (2012). Gps-tec variations during low solar activity period (2007-2009) at indian low latitude stations. *Astrophysics and Space Science*, *339*, 165–178. doi:10.1007/s10509-011-0973-6.

Lin, C. H., Lin, J. T., Chen, C. H., Liu, J. Y., Sun, Y. Y., Kakinami, Y., Matsumura, M., Chen, W. H., Liu, H., & Rau, R. J. (2014). Ionospheric shock waves triggered by rockets. *Annales Geophysicae*, *32*(9), 1145–1152. doi:10.5194/angeo-32-1145-2014.

Oka, M., Phan, T.-D., Eastwood, J. P., Angelopoulos, V., Murphy, N. A., Øieroset, M., Miyashita, Y., Fujimoto, M., McFadden, J., & Larson, D. (2011). Magnetic reconnection x-line retreat associated with dipolarization of the earth's magnetosphere. *Geophysical Research Letters*, *38*(20). doi:https://doi.org/10.1029/2011GL049350.

Rodríguez-Martínez, M., Pérez-Enríquez, H. R., Carrillo-Vargas, A., López-Montes, R., Araujo-Pradere, E. A., Casillas-Pérez, G. A., & Cruz-Abeyro, J. A. L. (2014). Ionospheric disturbances and their impact on ips using mexart observations. Sol Phys, *289*, 2677–2695. doi:https://doi.org/10.1007/s11207-014-0496-8.

Rumpf, C. M., Longenbaugh, R. S., Henze, C. E., Chavez, J. C., & Mathias, D. L. (2019). An algorithmic approach for detecting bolides with the geostationary lightning mapper. *Sensors*, *19*(5). URL: https://www.mdpi.com/1424-8220/19/5/1008. doi:10.3390/s19051008.

Sergeeva, M. A., Demyanov, V. V., Maltseva, O. A., Mokhnatkin, A., Rodriguez-Martinez, M., Gutierrez, R., Vesnin, A. M., Gatica-Acevedo, V. J., Gonzalez-Esparza, J. A., Fedorov, M. E., Ishina, T. V., Pazos, M., Gonzalez, L. X., Corona-Romero, P., Mejia-Ambriz, J. C., Gonzalez-Aviles, J. J., Aguilar-Rodriguez, E., Cabral-Cano, E., Mendoza, B., Romero-Hernandez, E., Caraballo, R., & Orrala-Legorreta, I. D. (2021). Assessment of morelian meteoroid impact on mexican environment. *Atmosphere*, *12*(2). doi:10.3390/atmos12020185.

Vázquez, M., Vaquero, J. M., Gallego, M. C., Roca Cortés, T., & Pallé, P. L. (2016). Long-Term Trends and Gleissberg Cycles in Aurora Borealis Records (1600 - 2015). Sol Phys, *291*(2), 613–642. doi:10.1007/s11207-016-0849-6.

Vlasov, M. N., & Kelley, M. C. (2010). Crucial discrepancy in the balance between extreme ultraviolet solar radiation and ion densities given by the international reference ionosphere model. *Journal of Geophysical Research: Space Physics*, *115*(A8). doi:https://doi.org/10.1029/2009JA015103.

Yang, Y.-M., Komjathy, A., Langley, R. B., Vergados, P., Butala, M. D., & Mannucci, A. J. (2014). The 2013 chelyabinsk meteor ionospheric impact studied using gps measurements. *Radio Science*, *49*(5), 341–350. doi:https://doi.org/10.1002/2013RS005344.

Zolesi, B., & Cander, L. R. (2014). *Ionospheric Prediction and Forecasting*.